Traffic gridlock on a honeycomb city

L. E. Olmos* and J. D. Muñoz†
Simulation of Physical Systems Group, Physics Department, National University of Colombia, Bogotá, Colombia
(Received 20 October 2016; published 31 March 2017)

Inspired by an old and almost in oblivion urban plan, we report the behavior of the Biham-Middleton-Levine (BML) model—a paradigm for studying phase transitions of traffic flow—on a hypothetical city with a perfect honeycomb street network. In contrast with the original BML model on a square lattice, the same model on a honeycomb does not show any anisotropy or intermediate states, but a single continuous phase transition between free and totally congested flow, a transition that can be completely characterized by the tools of classical percolation. Although the transition occurs at a lower density than for the conventional BML, simple modifications, like randomly stopping the cars with a very small probability or increasing the traffic light periods, drives the model to perform better on honeycomb lattices. As traffic lights and disordered perturbations are inherent in real traffic, these results question the actual role of the square gridlike designs and suggest the honeycomb topology as an interesting alternative for urban planning in real cities.

DOI: 10.1103/PhysRevE.95.032320

As cities turn denser, urban networks tend to adopt a squared-lattice shape [1], and many traditional urban planning styles, like the one Spaniards and Portugueses disseminated through all Latin America, are grounded on such square patterns [2]. Following this trend, most prominent studies on city traffic adopt square lattices [3–5]. Despite modern urban planners' claim that this design favors connectivity, the question of whether a square design optimizes traffic flow has not being studied systematically. In contrast, Nature usually opts for other alternatives. Hexagonal structures in two dimensions are present in cellular tissues [6,7], bee honeycombs [8], and soap bubbles [9,10]. Such patterns arise by minimizing surface energy on a fixed area [11]. Inspired by Nature, humans have also implemented hexagonal tesselations in a wide range of disciplines, including structured materials [12,13], wireless networks [14], computer graphics [15], etc. However, in the realm of the urban design, street patterns based upon hexagonal lock are just a theoretical alternative which has fallen into oblivion with almost no practical applications (see [16] and references therein), but hiding possible unexplored solutions for the overwhelming problem of traffic flow in modern cities.

The BML model is the simplest traffic cellular automaton able to exhibit self-organization, pattern formation, and phase transitions [17–20]. The original model describes two species of cars (east-running and north-running cars) moving by turns on a two-dimensional square lattice with periodic boundary conditions. Thus, the dynamics considers the city as a closed system with a constant number of cars and, does not allow cars to change direction. Despite these oversimplifications, the model allows us to focus on the nature of the phase transition between free and congested flow, and much extensive research has been based on it [3,21–23]. Driven by car density, the control parameter, the system falls into three different phases according to its asymptotic velocity v: free flow (all vehicles move $v = 1$), jammed phase (all vehicles are stuck $v = 0$), and intermediate states where jams and free flow coexist on a wide density range ($0 < v < 1$) [24–26]. A recent study has shown that such intermediate states are a consequence of the anisotropy inherent to the model [27], which produces two different phase transitions: one if the system is longer in the flow direction (longitudinal) and the other if the system is longer in the perpendicular one (transversal). It has also been reported that this intermediate phase disappears when some kind of randomization is introduced [25,28,29], or the traffic periods for the two cars are increased [30]. Some other extensions include free boundary conditions [31], four directions for the cars [32], or three-dimensional (3D) implementations [33]. In contrast, the role played by the network topology has been overlooked and, there are very few studies considering the Biham- Middleton-Levine (BML) model on different lattices: square lattice generalizations with extra sites in the bonds [34,35] and triangular lattices where three species of cars are considered [36,37]. In all cases a more complex behavior with different jammed phases is observed.

The main goal of this work is to test the BML traffic model [17] on honeycomb lattices. The intention is to explore how the topology (i.e., the node degree) affects the jamming transition and, eventually, when a honeycomb lattice offers a better performance than the square one. As in the original model, we will implement two car species moving by turns on a lattice with periodic boundary conditions, which can be closed on a torus in three different ways. Surprisingly, all systems show a single well-defined phase transition, although there is still a preferred flux direction and, moreover, there are cases where the BML performs better on honeycomb lattices than on square ones. So, this work questions the assumption that square grids are always optimal and suggests honeycombs as interesting alternatives for urban designers.

Model. Consider two types of cars moving zigzag in two different directions, yellow and black, on a honeycomblike lattice with periodic conditions (Fig. 1). Each node is connected with three others and can be in one of three states: empty, occupied by a yellow car, or occupied by a black one. The cars are initially randomly distributed over the lattice sites with spatial density ρ. The fully deterministic dynamics is as follows: On even (odd) steps, all yellow (black) cars attempt to advance one lattice site on their zigzag pattern. If the site ahead

*leolmoss@unal.edu.co
†jdmunozc@unal.edu.co

 ©2017 American Physical Society

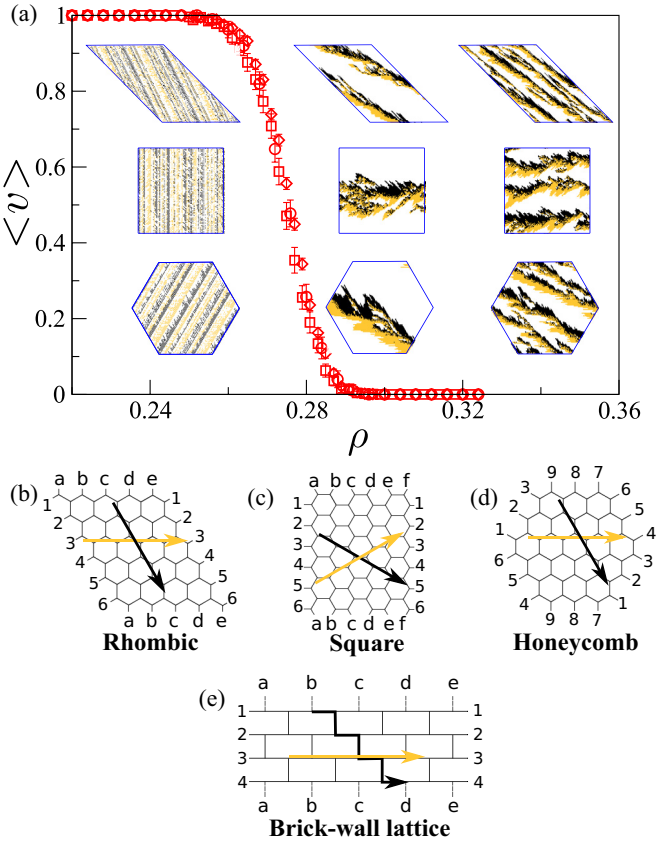

FIG. 1. Average velocity $\langle v\rangle$ vs density ρ (solid red line) for the BML model on 128×128 honeycomb lattices. Here and everywhere $\langle v\rangle$ is the fraction of random initial configurations with asymptotic velocity $v=1$. Insets show snapshots for free flow (left), one global jam (center), and random jams (right) on lattices with three boundaries: rhombic [diamonds and (b)], square [squares and (c)], and honeycomb [circles and (d)]. The flow direction is defined by just two (yellow and black arrows) of the three reflection symmetry axes. Topologically, the honeycomb lattice is equivalent to the brick-wall lattice (e).

of a car (in color direction) is currently empty, it advances; otherwise, it remains stationary. The system is implemented on a torus, i.e., with periodic boundary conditions, as in the original model. Nevertheless, there is no unique way to close a hexagonal lattice on a torus, but three [38]: square, rhombic, and honeycomb [Figs. 1(b)–1(d)]. We shall consider all these three tori in the most part of our analysis.

Absence of anisotropy. Starting the simulations from random configurations, the system reaches one of its limiting states after a transient period. If the system size is large enough ($L>64$), there are only two different limiting states [Fig. 1(a)]: a free-flow phase, where all cars move freely every time step ($v=1$) and a jammed phase, where no cars move ($v=0$). Contrary to the original model, there are no intermediate states, and the system exhibits a sharp jamming transition between these two phases [Fig. 1(a)].

As in the original model, there is a preferred flow direction: the one bisecting the two directions for cars and, in consequence, it could be possible to find a similar anisotropy in the correlation length. Let us start by studying the isotropy of

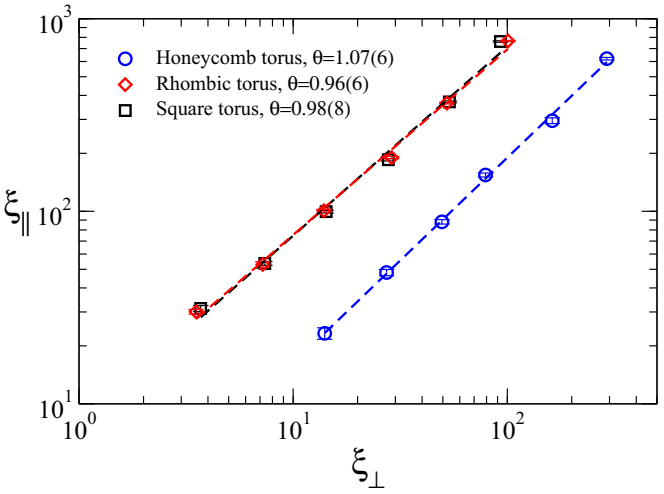

FIG. 2. Longitudinal $\xi_\parallel$ and transversal $\xi_\perp$ correlation lengths from final configurations at densities ρ in the range [0.265–0.310] for honeycomb lattices of different sizes with the three boundary conditions. Each point is an average over 50 configurations. The dashed lines show the power-law fits with anisotropy exponents $\theta\approx1.0$, i.e., the system behaves isotropic. Here and everywhere the error bars are 3σ.

the system. If the density is large enough, the system reaches a jamming state after a transient period. Following the methods applied in [27], we define the parallel (perpendicular) spatial correlation function [18] as

$$G_{\parallel(\perp)}(\vec{r}\,') = \frac{1}{N}\left\langle \sum_{\vec{r}} \sigma(\vec{r})\cdot\sigma(\vec{r}+\vec{r}\,')\right\rangle, \qquad (1)$$

where $\sigma(\vec{r})=1$ (0) if the site with position $\vec{r}$ is occupied (empty), N is the total number of cars and $\vec{r}\,'$ is a vector in the direction $\parallel$ ($\perp$) you want to compute the correlation function along. The symbol $\langle\rangle$ denotes averages over final jammed configurations starting from different random initial conditions at densities slightly above the jamming transition. The correlation functions are fitted with exponentials $G_{\parallel(\perp)}\propto\exp(-r/\xi_{\parallel(\perp)})$ to estimate the correlation lengths $\xi_{\parallel(\perp)}$ in each direction. The anisotropy exponent θ can be estimated numerically from the fact that, close to the critical point, the two correlation lengths must be related by $\xi_\parallel\sim\xi_\perp^\theta$ [39,40].

Figure 2 presents the correlation lengths computed from final configurations of the BML model for the three different honeycomb tori with different sizes and at densities close to the threshold transition. A power-law fit gives values for θ very close to 1, meaning that the system can be considered isotropic, such that the standard finite-size scaling (FSS) theory is suitable for describing the phase transition. Indeed, simulations on systems with different aspect ratios (not shown here) show no difference on the transition. This surprising result is, therefore, not a consequence of the preferred flow direction alone, but also of the grid itself.

The jamming transition. Figure 3(a) shows the transition curves for several system's sizes, ranging from $L=64$ to $L=1024$. In the honeycomb-torus case, the size L denotes the torus

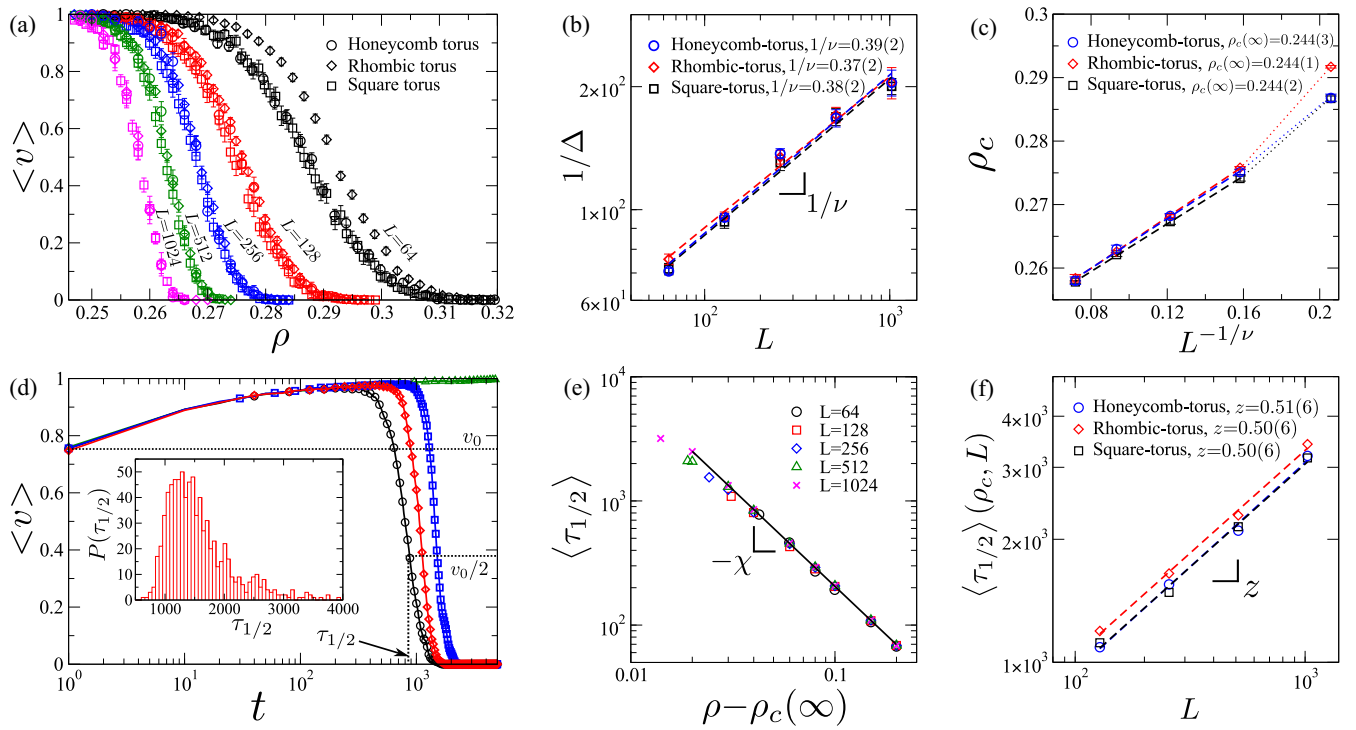

FIG. 3. Finite-size scaling analysis for the dynamical phase transition. (a) Transition curves for the three types of torus (symbols) with five different system sizes (colors), ranging from $L = 64$ to $L = 1024$. Each point is averaged over 2000 (1000) final configurations for $L \leqslant 512$ ($L = 1024$), obtained after convergence ($v = 0$ or $v = 1$) or after 2×10^5 time steps (whichever comes first). (b) Scaling of the transition width $\Delta(L)$. Dashed lines are power-law fits for the three tori, giving $1/\nu = 0.38(3)$ on average. (c) Scaling of the finite critical density. Because of strong finite-size effects, we neglect $L = 64$, and obtain $\rho_c(\infty) = 0.244(3)$ on average. (d) Average speed in function of time for five configurations. Dotted lines show the definition of the relaxation time $\tau_{1/2}$. The inset evidences that $\tau_{1/2}$ follows a log-normal distribution. (e) Mean relaxation time $\tau_{1/2}$ for densities above $\rho_c(\infty)$ on the honeycomb torus (results on other tori are quite similar). The slope gives on average a critical exponent $\chi = 1.55(2)$. (f) Scaling of the relaxation time at the critical point $\tau_{1/2}(\rho_c)$. On average, we obtain a dynamical critical exponent $z = 0.50(6)$. Each point on the last two figures is averaged over 100 configurations.

with the number of nodes closest to L^2.[1] As in many models with phase transitions in statistical physics (e.g., percolation [41]), the value of the critical density ρ_c decreases with system size, reaching a critical value ρ_c as the system size approaches infinity. By fitting the transition curves with an error function, Figs. 3(b) and 3(c) show that the transition width and the density threshold scale as [42]

$$\Delta(L) \sim L^{-1/\nu} \text{ and } |\rho_c - \langle\rho_c(L)\rangle| \sim L^{-1/\nu}. \qquad (2)$$

The values obtained for ν and $\rho_c(\infty)$ are very similar for the three tori. On average, we obtain $1/\nu = 0.38(3)$ and $\rho_c(\infty) = 0.244(3)$.

To investigate the dynamics of the model in the jammed state, let us define $\tau_{1/2}$ [18] as the time when the average speed is half of the initial speed [Fig. 3(d)]. This relaxation time follows a log-normal distribution and, therefore, its mean value can be estimated as $\langle\tau_{1/2}\rangle = \exp(\mu + \sigma^2/2)$, with $\mu \simeq \frac{1}{n}\sum_k \ln\tau_{1/2_k}$ and $\sigma^2 \simeq \frac{1}{n}\sum_k(\ln\tau_{1/2_k} - \mu)^2$. In the jammed phase ($\rho > \rho_c$), Fig. 3(e) shows that $\langle\tau_{1/2}\rangle$ is independent of the system size and scales as $\langle\tau_{1/2}\rangle \sim (\rho - \rho_c)^{-\chi}$ with $\chi = 1.55(2)$. In addition, the values of $\tau_{1/2}$ at the critical density ρ_c scales with system size as $\langle\tau_{1/2}\rangle(\rho_c, L) \sim L^z$, with $z = 0.50(6)$ [Fig. 3(f)]. The finite size scaling theory suggests that above the transition point $\chi/\nu = z = 0.56(5)$, in fair agreement with the value above.

A mean-field analysis. Interestingly, the critical density can be approximated by using a *naive* mean-field analysis, inspired by [43]. Consider the mean velocity of yellow cars (by symmetry, the reasoning is also valid for black cars). A yellow car will stop either because it is blocked by a black car or by another yellow car. On honeycomb lattices, there is almost no difference between these two types of interactions. At a random initial configuration, the probability that a car is blocked is ρ, that is, at the beginning of the simulation the proportion of stopped cars must be equal to ρ. Since black (yellow) cars spend on average a time $1/v$ on a site, they will reduce the speed of yellow cars from unity by ρ/v. Hence, a self-consistency equation for the average speed v will be

$$v = 1 - \frac{\rho}{v}, \qquad (3)$$

which gives ρ_c as the critical density at which the equation ceases to give a real solution. That occurs at $\rho_c = 0.25$, very close to the value of 0.244(3) obtained from finite size scaling.

[1] A honeycomb torus of size n has $6n^2$ nodes and n hexagons between the center and boundary. Thus, a L^2 torus actually corresponds to a torus in which n is the closest whole number of $L/\sqrt{6}$.

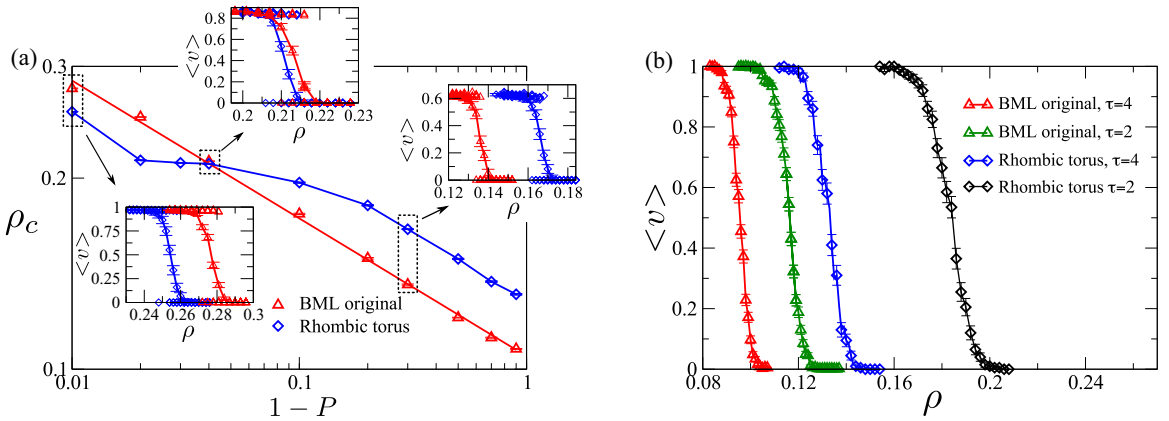

FIG. 4. Effects of two modifications of the BML model on both rhombic tori (diamonds) and square lattices (triangles). (a) Effect of including a random update, where cars move with probability P if the target site is empty. The figure shows the critical density ρ_c as a function of $1-P$ for lattice sizes $L=128$. Insets show the transition curves for three values of P. (b) Effect of increasing the traffic light period τ. The figure shows transition curves for $\tau=2$ and $\tau=4$ on lattices with size $L=256$. Each point in both figures is averaged on 400 runs. Measurements are obtained after 6×10^5 time steps or until convergence (whichever comes first).

A comparison with the square lattice. Remarkably, the critical density $\rho_c=0.244(3)$ for the BML model on a honeycomb is lower than the value of 0.283(2) for the lowest transition on a square lattice [27]. However, this order is reversed in at least two cases. First, let us remove full synchrony by introducing a random update [28], where a car advances with probability $P<1$ if the target site is empty; a modification that also destroys the intermediate state in of the BML model on square lattices [25,28,29]. Figure 4(a) compares the critical density of the model as function of $1-P$ on a rhombic torus with the one on a square lattice. The BML on a square lattice follows a power law behavior, with $\rho_c \propto (1-P)^{-0.22(1)}$, and behaves better only for a narrow interval. Below $P\approx0.96$, the honeycomb lattice overcomes the square one and behaves better, that is with a higher critical density.

Second, we have also studied the effect of increasing the traffic-light periods, that is cars on each direction have the chance to advance in τ consecutive time steps ($\tau=1$ for the original model), maintaining the parallel updating scheme. This also destroys the intermediate states on the original BML model and, furthermore, produces a spatial phase separation with small global speeds at intermediate densities [30]. Again, rhombic tori show higher critical densities than square lattices, even for $\tau=2$ or $\tau=4$ [Fig. 4(b)]. These results suggest that the model on a honeycomb is more resilient against small perturbations than on a square lattice.

Discussion. We have shown that the BML model with two flow directions behaves isotropically on honeycomb networks. There are no intermediate states, and a sharp transition from the moving phase to the jamming phase is observed at a critical vehicle density. Despite the fact that there is a preferred flow direction, the correlation length shows to be isotropic. This surprising result may be a consequence of the symmetries of the honeycomb. Indeed, it has been shown that high-order tensors on a hexagonal lattice (the dual lattice of a honeycomb) are isotropic up to second order in the grid size [44]. Whether this is the reason for such isotropy or not will be an interesting subject of future research.

By performing a classical scaling analysis, we characterized completely the transition, measuring the critical density and three critical exponents. Although the model shows a lower critical density than on square lattices, this issue is reversed by introducing small and simple perturbations, like increasing the traffic light periods or including a random update with very low probabilities to brake. Street patterns based upon hexagonal blocks were proposed by several planners in the early 20th century [16]. Despite urban designers demonstrating the economic advantages and efficient land use of hexagonal plans, this idea never ceased to be a theoretical alternative to the rectangular grid, never implemented in urban street patterns. Furthermore, the contemporary movements of new urbanism claims that square grid layouts increase the connectivity,[2] dispersing traffic and reducing driving times, because they are assumed to be mixed use, walkable, and more pedestrian friendly. However, such assumptions are criticized by practical considerations [16]. Indeed, empirical data about safety [45,46] suggest that four-leg intersections, ubiquitous in square grids, increase both the number of crashes and injuries significantly, suggesting to reconsider urban residential layouts where T junctions and dead ends predominate (*cul de sac*, radburn, fused grid). This is why city planners use to restrict flow direction emulating T junctions, even at the cost of reducing connectivity. Although those issues are usually thought of in a highways network, they also apply to residential neighborhoods, because residential and working areas mix as cities become denser and, real-time traffic applications push cars into residential areas to avoid jams. This is the case in many Latin American cities. Thus, honeycomb grids emerge as a unifying idea, i.e., T junctions plus connectivity.

Our results suggest that the BML model on hexagons under perturbations is more robust than on squares. Since the included perturbations, i.e., traffic lights and disorder,

[2]See http://www.newurbanism.org/.

are crucial in real traffic, this work questions the real role of square gridlike designs and supports honeycombs as an interesting alternative for urban densification processes. Regarding practical applications, a honeycomb lattice can be mapped into a brick-wall lattice [see Fig. 1(e)] which, in turn, can be derived from the square lattice by eliminating bonds. Thus, instead of an improbable reconstruction of the city, we could emulate the honeycomb topology by restricting the flow in certain road segments. Of course, our model oversimplifies the city, as most previous BML models do. A real city is an open system, with cars entering and leaving the flux all the time, as described by empirical origin-destination matrices and the incoming flux as control parameter. Testing a honeycomb network against a square one in that context would be a beautiful subject of future work and a further contribution of statistical physics to the urbanism theory.

Acknowledgments. We thank the Complex Systems Research Center CeiBA-Complejidad and the National University of Colombia for financial support. We are indebted M. C. González for hospitality and useful discussions.

[1] E. Strano, V. Nicosia, V. Latora, S. Porta, and M. Barthelemy, Sci. Rep. **2**, 296 (2012).
[2] A. Rama, *The Lettered City* (Ediciones del Norte, Hanover, NH, 2002).
[3] D. Chowdhury, L. Santen, and A. Schadschneider, Phys. Rep. **329**, 199 (2000).
[4] A. Mazloumian, N. Geroliminis, and D. Helbing, Philos. Trans. R. Soc. A **368**, 4627 (2010).
[5] M. Li, Z.-J. Ding, R. Jiang, M.-B. Hu, and B.-H. Wang, J. Stat. Mech. (2011) P12001.
[6] J. C. M. Mombach, M. A. Z. Vasconcellos, and R. M. C. de Almeida, J. Phys. D: Appl. Phys. **23**, 600 (1990).
[7] A. B. Patel, W. T. Gibson, M. C. Gibson, and R. Nagpal, PLoS Comput. Biol. **5**, e1000412 (2009).
[8] C. W. W. Pirk, H. R. Hepburn, S. Radloff, and J.Tautz, Naturwissenschaften **91**, 350 (2004).
[9] D. Weaire, Contemp. Phys. **25**, 59 (1984).
[10] D. Weaire, *The Kelvin Problem* (Taylor and Francis, London, 1996).
[11] J. von Neumann, in *Metal Interfaces* (American Society for Metals, Cleveland, 1952), p. 108.
[12] R. Oftadeh, B. Haghpanah, D. Vella, A. Boudaoud, and A. Vaziri, Phys. Rev. Lett. **113**, 104301 (2014).
[13] L. J. Gibson and M. F. Ashby, *Cellular Solids: Structure and Properties* (Cambridge University Press, Cambridge, England, 1999).
[14] R. H. Frenkiel, US Patent No. 4,144,411, March 13, 1979.
[15] C. Jiang, J. Wang, J. Wallner, and H. Pottmann, Computer Graphics Forum **33**, 185 (2014).
[16] E. Ben-Joseph and D. Gordon, J. Urban Des. **5**, 237 (2000).
[17] O. Biham, A. A. Middleton, and D. Levine, Phys. Rev. A **46**, R6124 (1992).
[18] S. I. Tadaki and M. Kikuchi, Phys. Rev. E **50**, 4564 (1994).
[19] J. Torok and J. Kertész, Physica A **231**, 515 (1996).
[20] H. S. Gupta and R. Ramaswamy, J. Phys. A: Math. Gen. **29**, L547 (1996).
[21] J.-R. Xie, R. Jiang, Z.-J. Ding, Q.-L. Li, and B.-H. Wang, Phys. Rev. E **87**, 022812 (2013).
[22] Y. Sun and I. Timofeyev, Phys. Rev. E **89**, 052810 (2014).
[23] T. Nagatani, Rep. Prog. Phys. **65**, 1331 (2002).
[24] R. M. D'Souza, Phys. Rev. E **71**, 066112 (2005).
[25] R. M. D'Souza, Complexity **12**, 30 (2006).
[26] W. K. Yung, Master's thesis, University of Hong Kong, Department of Physics, 1998, http://hub.hku.hk/handle/10722/33474.
[27] L. E. Olmos and J. D. Muñoz, Phys. Rev. E **91**, 050801 (2015).
[28] Z.-J. Ding, R. Jiang, W. Huang, and B.-H. Wang, J. Stat. Mech. (2011) P06017.
[29] Z.-J. Ding, R. Jiang, and B.-H. Wang, Phys. Rev. E **83**, 047101 (2011).
[30] D. Sun, R. Jiang, and B.-H. Wang, Comput. Phys. Commun. **181**, 301 (2010).
[31] S. I. Tadaki, Phys. Rev. E **54**, 2409 (1996).
[32] D. Huang and W. Huang, Physica A **370**, 747 (2006).
[33] H. F. Chau and K. Y. Wan, Phys. Rev. E **60**, 5301 (1999).
[34] T. Horiguchi and T. Sakakibara, Physica A **252**, 388 (1998).
[35] T. Sakakibara, Y. Honda, and T. Horiguchi, Physica A **276**, 316 (2000).
[36] T. Nagatani, Physica A **271**, 200 (1999).
[37] J. C. García, S. Rodríguez, and F. Sancho, in *Proceedings of the European Conference on Complex Systems* (Springer International Publishing, Switzerland, 2013), pp. 943–948.
[38] I. Stojmenovic, IEEE Trans. Parallel Distrib. Syst. **8**, 1036 (1997).
[39] K. Binder and J.-S. Wang, J. Stat. Phys. **55**, 87 (1989).
[40] S. Redner and P. R. Mueller, Phys. Rev. B **26**, 5293 (1982).
[41] D. Stauffer and A. Aharony, *Introduction to Percolation Theory* (Taylor & Francis, London, 1992).
[42] M. D. Rintoul and S. Torquato, J. Phys. A: Math. Gen. **30**, L585 (1997).
[43] B. H. Wang, Y. F. Woo, and P. M. Hui, J. Phys. A **8**, 1036 (1996).
[44] S. Wolfram, J. Stat. Phys. **45**, 471 (1986).
[45] E. Dumbaugh and R. Rae, J. Am. Plann. Assoc. **75**, 309 (2009).
[46] J. Sun and G. Lovegrove, Can. J. Civil Eng. **40**, 35 (2013).